Link Lengths Optimization Based on Multiple Performance Indexes of Anthropomorphic Manipulators

QINHUAN XU, QIANG ZHAN, AND XINYANG TIAN
Robotics Institute, Beihang University, Beijing 100191, China

Corresponding author: Qiang Zhan (qzhan@buaa.edu.cn)

ABSTRACT How to determine the optimal link length parameters according to task requirements and constraints is a key problem in the design of anthropomorphic manipulators. Considering multiple performance indexes such as dexterity and end stiffness, this article presents a method on how to maximally improve the comprehensive motion performance of anthropomorphic manipulators by optimizing the link lengths. Firstly, the joint motion ranges of human arm are obtained through analyzing the motion mechanism and the motion forms. Then the kinematics model of manipulators with the optimal configuration is established by using screw theory, and a comprehensive evaluation index for the motion performance is proposed by considering the Jacobian matrix condition number, manipulability, and end stiffness. Taking the evaluation index as the objective function, the corresponding constraints and the optimization model are established to optimize the link lengths of manipulators with both flexibility and stiffness. Through comparative analyses, it can be seen that the global comprehensive performance index value of the optimized anthropomorphic manipulators increases by about 23.97%, and the motion performance is significantly improved.

INDEX TERMS Anthropomorphic manipulator, end stiffness, comprehensive motion performance, evaluation index, link length optimization.

I. INTRODUCTION

As a great product of long-term natural evolution, human arm can flexibly complete various complex and precise movements, which are mainly resulted from its complex physiological mechanisms. The mechanisms of human arm are difficult to be described completely by precise mathematical models or structural models [1], [2]. Therefore, how to use a reasonable structure to achieve the similar operation function of human arm as much as possible is a key problem to be solved in the design process of anthropomorphic manipulators. Constrained by the working environment and the mechanical structure, the overall length of anthropomorphic manipulators is often limited to a certain extent, which affects the motion performance greatly [3], [4]. On the premise of satisfying constraints, to improve the motion performance through optimizing link lengths of anthropomorphic manipulators has become a necessary work in the design process.

The associate editor coordinating the review of this manuscript and approving it for publication was Guilin Yang.

In order to better simulate the operation of human arm, anthropomorphic manipulators should both have good flexibility and ensure precise end trajectory. Therefore, the flexibility and stiffness performance of anthropomorphic manipulators have become the main references for the optimization of the link length parameters [5]. For improving the flexibility of anthropomorphic manipulators, some scholars have used Jacobian matrix condition number [6]–[8] and manipulability [9], [10] as the evaluation indexes of the link length parameters, and studied the manipulator's scale synthesis problem with the optimal flexibility. On this basis, Hwang and Yoon [11], Hwang *et al.* [12], and Lim *et al.* [13] optimized the link length parameters of seven DOFs (degrees of freedom) manipulators with genetic algorithm by using STL (structural length index), GCI (global conditioning index) and improved dynamic condition number as the design indexes. In addition, Liu *et al.* [14] revealed the variation rule of the reachable workspace of a manipulator with the scale parameters and joint motion ranges, and used the reciprocal of Jacobian matrix condition number as the performance evaluation index to synthesize a group of optimal structural

TABLE 1. Motion forms and motion range of human arm.

Joint	DOF(s)	Motion Forms	Motion range
Shoulder Joint	3	forward bending and backward stretching	90°~150°、30°~40°
		abduction and adduction	80°~90°、20°~40°
		inward and outward rotation	45°~60°、45°~70°
Elbow Joint	1	flexion and hyperextension	135°~150°、0°~10°
Wrist Joint	3	extension and flexion	35°~60°、50°~60°
		radial flexion and ulnar flexion	25°~30°、30°~40°
		anterior and posterior rotation	80°~90°、80°~90°

scale parameters. Mayorga *et al.* [15] presented a simple index for manipulator kinematic design optimization and best posture determination that was derived by establishing a simple upper bound for the change rate of an isotropic condition. Liu *et al.* [16] optimized the link length parameters of a manipulator based on performance evaluation indexes such as workspace, singularity and isotropy.

Based on stiffness performance optimization of serial manipulators, some scholars have made relevant researches. Ajoudani *et al.* [17] took the shape and size of stiffness ellipsoid as the evaluation index of stiffness performance. The shape and size of stiffness ellipsoid are changed by optimizing the structural parameters of manipulators, which made the stiffness ellipsoid have the maximum component in the direction of loading. Chen *et al.* [18] analyzed how to improve the stiffness by optimizing the length and configuration of manipulators based on the static stiffness model. A global stiffness performance index is proposed and used as the objective function to optimize the link lengths of a manipulator. In order to improve the stiffness characteristics of a serial milling manipulator, Zhang *et al.* [19] established a comprehensive stiffness performance optimization model based on the kinematics model and Jacobian matrix, and optimized the length parameters and poses of a manipulator. Jiao *et al.* [20] designed a comprehensive stiffness performance evaluation index for a six-DOF serial robot based on the static stiffness model, and proposed an offline posture optimization method. Chen *et al.* [21] analyzed the cartesian stiffness of a rope-driven seven-DOF anthropomorphic manipulator and proposed an optimization algorithm to improve the stiffness performance of the manipulator during movement.

For the optimization design of anthropomorphic manipulators' link length parameters, most researches are only carried out from one aspect of flexibility or stiffness performance. If the flexibility of a manipulator in the workspace are excessively pursued, the stiffness will be reduced to a certain extent, which affects its motion accuracy and dynamic characteristics. However, only the stiffness performance is used as the evaluation index to optimize the link lengths, which cannot guarantee the flexibility of a manipulator [22]. Therefore, in order to balance the flexibility and stiffness performance of anthropomorphic manipulators, this article designs a comprehensive performance evaluation index considering the Jacobian matrix condition number, manipulability and end stiffness, and gives an optimization method for

anthropomorphic manipulators' link lengths. The optimization method provides theoretical basis and foundation for the design of anthropomorphic manipulators with both flexibility and stiffness.

The remainder of this article is organized as follows. In section II, the motion mechanism and configuration of human arm are analyzed. In section III, a comprehensive evaluation index of anthropomorphic manipulators is proposed. In section IV, the optimization of anthropomorphic manipulators is completed. Finally, conclusions of the paper are given in section V.

II. MOTION MECHANISM AND CONFIGURATION ANALYSIS OF HUMAN ARM
A. MOTION MECHANISM ANALYSIS OF HUMAN ARM
It is necessary to analyze the motion mechanism of human arm for the development of anthropomorphic manipulators. In human motion anatomy, human arm consists of the shoulder joint, upper arm, elbow joint, forearm and wrist joint from top to bottom, and its motion mainly comes from the motions of joints. Human arm is usually simplified as a mechanism of seven DOFs, including three DOFs of the shoulder joint, one DOF of the elbow joint and three DOFs of the wrist joint [23], [24].

The shoulder joint of human arm is a typical ball-and-socket joint, which is the most flexible joint in human body. Its motion forms include forward bending and backward stretching, abduction and adduction, inward and outward rotation. The elbow joint is a single DOF rotatory joint, which can realize the flexion and hyperextension of human arm. The wrist joint is composed of a radial joint and a carpal joint. Since the two joints can move independently of each other, the wrist joint can be regarded as consisting of a ring-axis joint with single DOF and a condyle joint with two DOFs. The motion forms of the wrist joint include extension and flexion, radial flexion and ulnar flexion, anterior and posterior rotation. The motion forms and corresponding motion ranges of human arm can be obtained through actual measurement and data analysis, as shown in Table 1.

B. CONFIGURATION ANALYSIS OF HUMAN ARM
The basic starting point for the development of an anthropomorphic manipulator is to make it more flexible and adaptable in the working environment, so as to achieve similar operating functions and workspace as human arm. Restricted by the mechanical structure, it is difficult to completely copy the
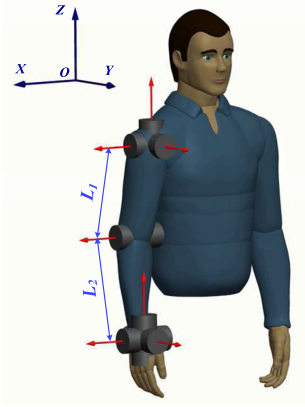
FIGURE 1. Simplified kinematics model of human arm.

structure of human arm. Each joint of human arm can be equivalent to a mechanical motion pair with the same motion form, and then a reasonable scheme can be selected for the design according to the specific configuration. At present, the configuration with seven DOFs is mostly adopted with three serial rotatory joints for the shoulder joint, one rotatory joint for the elbow joint, and three serial rotatory joints for the wrist joint. The structure model is shown in FIGURE 1, where L_1 and L_2 respectively represent the lengths of the upper arm and the forearm.

For the seven DOFs human arm structure, there are different configurations of anthropomorphic manipulators with different joint settings, among which the one shown in FIGURE 2 is regarded as the optimal one. Compared with the most widely used manipulator configuration with 6 DOFs, this configuration adds a rotary joint 3 along the common normal direction of the two parallel axes between joints 2 and 4 [25].

III. PERFORMANCE EVALUATION INDEXES OF ANTHROPOMORPHIC MANIPULATORS

The anthropomorphic manipulators with seven DOFs can not only eliminate the singular configuration in the workspace, but also avoid joint limits and space obstacles flexibly, so as to realize the operation posture and functions of human arm. After determining the configuration, evaluating and optimizing the link length parameters combined with task requirements is a key step in the design process of anthropomorphic manipulators. This article proposes a comprehensive evaluation index considering Jacobian matrix condition number, manipulability and stiffness performance, and completes the link length parameters optimization of anthropomorphic manipulators with seven DOFs.

A. FORWARD KINEMATICS MODELING OF ANTHROPOMORPHIC MANIPULATORS

For the anthropomorphic manipulators' configuration shown in FIGURE 2, the link lengths are assumed to be l_1, l_2, l_3, l_4, l_5, l_6, l_7, as shown in FIGURE 3, where, $d_1 = l_1 + l_2$, $d_2 = l_3 + l_4$, $d_3 = l_5 + l_6$ and $d_4 = l_7$.

The kinematics model of the anthropomorphic manipulator is established using screw theory. First, establish the base
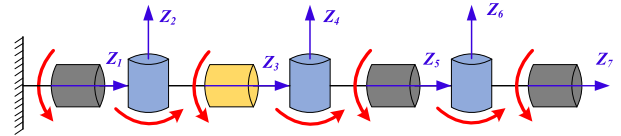

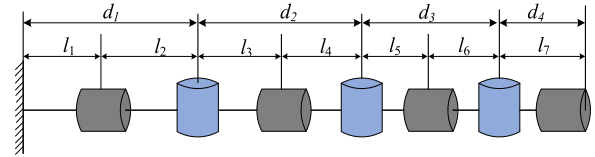**FIGURE 2.** An optimal configuration of anthropomorphic manipulator.

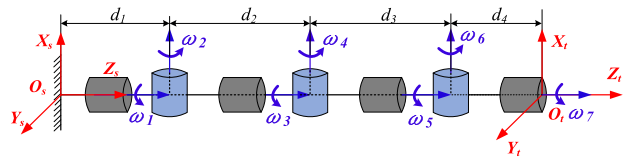**FIGURE 3.** Link parameters of anthropomorphic manipulator.

FIGURE 4. Screw coordinates of anthropomorphic manipulator.

coordinate system $O_s - X_s Y_s Z_s$ and the end coordinate system $O_t - X_t Y_t Z_t$, as shown in FIGURE 4, where $\boldsymbol{\omega}_i$ is the unit vector of the rotation axis corresponding to joint i.

The homogeneous matrix of the initial pose of the manipulator is obtained as

$$\boldsymbol{g}_{st}(0) = \begin{bmatrix} \boldsymbol{R}_{st}(0) & \boldsymbol{P}_{st}(0) \\ 0 & 1 \end{bmatrix} = \begin{bmatrix} 1 & 0 & 0 & 0 \\ 0 & 1 & 0 & 0 \\ 0 & 0 & 1 & d_1 + d_2 + d_3 + d_4 \\ 0 & 0 & 0 & 1 \end{bmatrix} \quad (1)$$

The unit vector of rotation axis corresponding to joint i is $\boldsymbol{\omega}_i = (\omega_{ix}, \omega_{iy}, \omega_{iz})^T$ and the position vector is $\boldsymbol{q}_i = (q_{ix}, q_{iy}, q_{iz})^T$, then the corresponding motion screw coordinate $\boldsymbol{\xi}_i$ can be expressed as

$$\boldsymbol{\xi}_i = \begin{bmatrix} \boldsymbol{v}_i \\ \boldsymbol{\omega}_i \end{bmatrix} = \begin{bmatrix} -\boldsymbol{\omega}_i \times \boldsymbol{q}_i \\ \boldsymbol{\omega}_i \end{bmatrix} \in \boldsymbol{R}^{6\times1}, (i = 1, 2 \cdots 7) \quad (2)$$

The motion screw coordinate $\boldsymbol{\xi}_i$ of each joint is calculated, as shown in Table 2.

$\boldsymbol{\xi}_i \in \boldsymbol{R}^{6\times1}$ is the Plücker coordinate of the unit motion screw. The motion screw $\hat{\boldsymbol{\xi}}_i$ can be calculated using the inverse operator $\wedge$ according to the motion screw coordinate of each joint.

$$\hat{\boldsymbol{\xi}}_i = \begin{bmatrix} \boldsymbol{v}_i \\ \boldsymbol{\omega}_i \end{bmatrix}^\wedge = \begin{bmatrix} \hat{\boldsymbol{\omega}}_i & \boldsymbol{v}_i \\ 0 & 0 \end{bmatrix} \quad (3)$$

where, $\hat{\boldsymbol{\xi}}_i \in se(3)$ is the 4×4 matrix form of the motion screw coordinate, which is located in the Lie algebra $se(3)$ corresponding to the special Euclidean group $SE(3)$. $\hat{\boldsymbol{\omega}}_i \in so(3)$ is the 3×3 antisymmetric matrix form of the joint axis unit vector, located in the Lie algebra $so(3)$ corresponding to the special orthogonal group $SO(3)$, and its expression is

$$\hat{\boldsymbol{\omega}} = \begin{bmatrix} 0 & -\omega_z & \omega_y \\ \omega_z & 0 & -\omega_x \\ -\omega_y & \omega_x & 0 \end{bmatrix} \in so(3) \in \boldsymbol{R}^{3\times3} \quad (4)$$

TABLE 2. Motion screw coordinate of each joint.

Joint angle θ_i	Axis vector ω_i	Position vector q_i	Screw coordinates $\xi_i = [v_i, \omega_i]^{\mathrm{T}}$
θ_1	$\omega_1 = (0,0,1)^{\mathrm{T}}$	$q_1 = (0,0,d_1)^{\mathrm{T}}$	$\xi_1 = (0,0,0,0,0,1)^{\mathrm{T}}$
θ_2	$\omega_2 = (1,0,0)^{\mathrm{T}}$	$q_2 = (0,0,d_1)^{\mathrm{T}}$	$\xi_2 = (0,d_1,0,1,0,1)^{\mathrm{T}}$
θ_3	$\omega_3 = (0,0,1)^{\mathrm{T}}$	$q_3 = (0,0,d_1)^{\mathrm{T}}$	$\xi_3 = (0,0,0,0,0,1)^{\mathrm{T}}$
θ_4	$\omega_4 = (1,0,0)^{\mathrm{T}}$	$q_4 = (0,0,d_1+d_2)^{\mathrm{T}}$	$\xi_4 = (0,d_1+d_2,0,1,0,0)^{\mathrm{T}}$
θ_5	$\omega_5 = (0,0,1)^{\mathrm{T}}$	$q_5 = (0,0,d_1+d_2+d_3)^{\mathrm{T}}$	$\xi_5 = (0,0,0,0,0,1)^{\mathrm{T}}$
θ_6	$\omega_6 = (1,0,0)^{\mathrm{T}}$	$q_6 = (0,0,d_1+d_2+d_3)^{\mathrm{T}}$	$\xi_6 = (0,d_1+d_2+d_3,0,1,0,0)^{\mathrm{T}}$
θ_7	$\omega_7 = (0,0,1)^{\mathrm{T}}$	$q_7 = (0,0,d_1+d_2+d_3)^{\mathrm{T}}$	$\xi_7 = (0,0,0,0,0,1)^{\mathrm{T}}$

The exponential form of the pose matrix is

$$e^{\hat{\omega}\theta} = I + \hat{\omega}\theta + \frac{(\hat{\omega}\theta)^2}{2!} + \frac{(\hat{\omega}\theta)^3}{3!} + \cdots$$
$$= I + \hat{\omega}\sin\theta + \hat{\omega}^2(1-\cos\theta) \quad (5)$$

The exponential form of the motion screw matrix is

$$e^{\hat{\xi}\theta} = \begin{cases} \begin{bmatrix} e^{\hat{\omega}\theta} & (I - e^{\hat{\omega}\theta})(\omega \times v) + \omega\omega^T v\theta \\ 0 & 1 \end{bmatrix}, \omega \neq 0 \\ \begin{bmatrix} I & v\theta \\ 0 & 1 \end{bmatrix}, \omega = 0 \end{cases} \quad (6)$$

According to the above formula, the exponential product corresponding to each joint is obtained.

$$e^{\hat{\xi}_1\theta_1} = \begin{bmatrix} \cos\theta_1 & -\sin\theta_1 & 0 & 0 \\ \sin\theta_1 & \cos\theta_1 & 0 & 0 \\ 0 & 0 & 1 & 0 \\ 0 & 0 & 0 & 1 \end{bmatrix}$$

$$e^{\hat{\xi}_2\theta_2} = \begin{bmatrix} 1 & 0 & 0 & 0 \\ 0 & \cos\theta_2 & -\sin\theta_2 & d_1\sin\theta_2 \\ 0 & \sin\theta_2 & \cos\theta_2 & d_1(1-\cos\theta_2) \\ 0 & 0 & 0 & 1 \end{bmatrix}$$

$$e^{\hat{\xi}_3\theta_3} = \begin{bmatrix} \cos\theta_3 & -\sin\theta_3 & 0 & 0 \\ \sin\theta_3 & \cos\theta_3 & 0 & 0 \\ 0 & 0 & 1 & 0 \\ 0 & 0 & 0 & 1 \end{bmatrix}$$

$$e^{\hat{\xi}_4\theta_4} = \begin{bmatrix} 1 & 0 & 0 & 0 \\ 0 & \cos\theta_4 & -\sin\theta_4 & (d_1+d_2)\sin\theta_4 \\ 0 & \sin\theta_4 & \cos\theta_4 & (d_1+d_2)(1-\cos\theta_4) \\ 0 & 0 & 0 & 1 \end{bmatrix}$$

$$e^{\hat{\xi}_5\theta_5} = \begin{bmatrix} \cos\theta_5 & -\sin\theta_5 & 0 & 0 \\ \sin\theta_5 & \cos\theta_5 & 0 & 0 \\ 0 & 0 & 1 & 0 \\ 0 & 0 & 0 & 1 \end{bmatrix}$$

$$e^{\hat{\xi}_6\theta_6} = \begin{bmatrix} 1 & 0 & 0 & 0 \\ 0 & \cos\theta_6 & -\sin\theta_6 & (d_1+d_2+d_3)\sin\theta_6 \\ 0 & \sin\theta_6 & \cos\theta_6 & (d_1+d_2+d_3)(1-\cos\theta_6) \\ 0 & 0 & 0 & 1 \end{bmatrix}$$

$$e^{\hat{\xi}_7\theta_7} = \begin{bmatrix} \cos\theta_7 & -\sin\theta_7 & 0 & 0 \\ \sin\theta_7 & \cos\theta_7 & 0 & 0 \\ 0 & 0 & 1 & 0 \\ 0 & 0 & 0 & 1 \end{bmatrix}$$

The kinematics forward solution of the manipulator is

$$g_{st}(\theta) = e^{\hat{\xi}_1\theta_1} e^{\hat{\xi}_2\theta_2} \cdots e^{\hat{\xi}_7\theta_7} g_{st}(0) = \begin{bmatrix} R & P \\ 0 & 1 \end{bmatrix} \quad (7)$$

The Jacobian matrix J represents the linear transformation relationship between the end velocity $v(\theta)$ and the joint velocity $\dot{\theta}$ of the manipulator.

$$v(\theta) = J\dot{\theta} \quad (8)$$
$$J = [\xi_1', \xi_2', \xi_3' \cdots, \xi_i', \cdots \xi_7'] \quad (9)$$

where, $\xi_i' = \begin{bmatrix} -\omega_i' \times p_i' \\ \omega_i' \end{bmatrix}$;

$$\omega_i' = \left(\prod_{s=1}^{i-1} e^{\hat{\omega}_s\theta_s}\right)\omega_i = e^{\hat{\omega}_1\theta_1} e^{\hat{\omega}_2\theta_2} \cdots e^{\hat{\omega}_{i-1}\theta_{i-1}}\omega_i;$$

$$p_i' = \left(\prod_{s=1}^{i-1} e^{\hat{\omega}_s\theta_s}\right)p_i = e^{\hat{\omega}_1\theta_1} e^{\hat{\omega}_2\theta_2} \cdots e^{\hat{\omega}_{i-1}\theta_{i-1}}p_i.$$

B. ESTABLISHMENT OF PERFORMANCE EVALUATION INDEXES FOR ANTHROPOMORPHIC MANIPULATOR

Since the Jacobian matrix J represents the mapping relationship between the end operation velocity and the joint velocities, the algebraic eigenvalues of the Jacobian matrix J (such as determinant, condition number, maximum and minimum singular values, etc.) are usually used as the index to evaluate flexibility of the anthropomorphic manipulator. In order to ensure the motion accuracy and dynamic performance, it is necessary to consider the stiffness performance of the manipulator at the same time. The stiffness matrix changes with the change of the Jacobian matrix, so the end stiffness has an important correlation with the pose and link lengths of the manipulator. In this article, the flexibility performance index and the stiffness performance index are synthesized, and a comprehensive performance index considering the Jacobian matrix condition number, manipulability and end stiffness of the anthropomorphic manipulator is designed.

1) JACOBIAN MATRIX CONDITION NUMBER

The variation range of the Jacobian matrix condition number k is $[1, +\infty)$, and the closer k is to 1, the better the isotropic of the manipulator motion and the more uniform the velocity ratio. The dexterity of the manipulator reaches the maximum

when $k = 1$ [26]. Since the dimensions of the elements representing translation and rotation in the Jacobian matrix are different, this article uses the characteristic length method to make it reach the normalized length. The Frobennius norm is used to measure the Jacobian matrix of the anthropomorphic manipulator so as to construct a normalized Jacobian matrix condition number. The condition number is defined as

$$k_F = \frac{1}{6}\sqrt{tr\left(JJ^{\mathrm{T}}\right) tr\left[\left(JJ^{\mathrm{T}}\right)^{-1}\right]} \qquad (10)$$

2) MANIPULABILITY ANALYSIS OF ANTHROPOMORPHIC MANIPULATOR

In order to quantitatively describe the flexibility of manipulator, Yoshikawa [27] defined the manipulability $w = \sqrt{\det\left(JJ^{\mathrm{T}}\right)}$, which represents a comprehensive measure of the motion ability in various directions. Manipulability can be used to evaluate the overall flexibility of a manipulator. When $w = 0$, the manipulator is in a singular configuration; when $w > 0$, the manipulator is in a non-singular configuration; when $w = +\infty$, the manipulator is in an indeterminate configuration. The larger w is, the better flexibility the manipulator has. The manipulability can directly reflect the proximity of the manipulator to singular configuration and indeterminate configuration.

3) STATIC STIFFNESS ANALYSIS OF ANTHROPOMORPHIC MANIPULATOR

In the design process of anthropomorphic manipulator, the end stiffness is also an important performance evaluation index. The end stiffness matrix depends on the joint stiffness and the Jacobian matrix [28], [29]. The stiffness of joint i of the manipulator with n DOFs is represented by K_{qi} $(i = 1, 2, \cdots, n)$, and the joint stiffness matrix $\boldsymbol{K}_q$ is denoted as

$$\boldsymbol{K}_q = diag\left(K_{q1}, K_{q2}, \cdots, K_{qn}\right) \qquad (11)$$

The Jacobian matrix is $\boldsymbol{J} \in \boldsymbol{R}^{6 \times 7}$ for the manipulator with seven DOFs, and the end stiffness matrix $\boldsymbol{K}$ can be expressed by the generalized inverse of the Jacobian matrix $\boldsymbol{J}^+$:

$$\boldsymbol{K} = (\boldsymbol{J}^+)^{\mathrm{T}}\boldsymbol{K}_q\boldsymbol{J}^+ \qquad (12)$$

Substitute $\boldsymbol{J}^+ = \boldsymbol{J}^{\mathrm{T}}(\boldsymbol{J}\boldsymbol{J}^{\mathrm{T}})^{-1}$ into Equation (12), we can get

$$\boldsymbol{K} = (\boldsymbol{J}^{\mathrm{T}}(\boldsymbol{J}\boldsymbol{J}^{\mathrm{T}})^{-1})^{\mathrm{T}}\boldsymbol{K}_q\boldsymbol{J}^{\mathrm{T}}(\boldsymbol{J}\boldsymbol{J}^{\mathrm{T}})^{-1} \qquad (13)$$

After simplification

$$\boldsymbol{K} = (\boldsymbol{J}\boldsymbol{J}^{\mathrm{T}})^{-\mathrm{T}}\boldsymbol{J}K_q\boldsymbol{J}^{\mathrm{T}}(\boldsymbol{J}\boldsymbol{J}^{\mathrm{T}})^{-1} \qquad (14)$$

It can be seen that the stiffness matrix $\boldsymbol{K}$ is a Hermite matrix, $K^{\mathrm{H}} = K$. Taking any non-zero vector $\boldsymbol{B} \in \boldsymbol{R}^{6 \times 1}$, the Rayleigh quotient [18] of the stiffness matrix $\boldsymbol{K}$ is

$$R(\boldsymbol{B}) = \frac{\boldsymbol{B}^{\mathrm{H}}\boldsymbol{K}\boldsymbol{B}}{\boldsymbol{B}^{\mathrm{H}}\boldsymbol{B}} \qquad (15)$$

Assume that the force vector of the anthropomorphic manipulator end is $\boldsymbol{F}$ and the deformation vector is $\boldsymbol{X}$, so the ratio of the modulus square of $\boldsymbol{F}$ to the modulus square of $\boldsymbol{X}$

can be expressed by using the Rayleigh quotient of the matrix $\boldsymbol{K}^{\mathrm{T}}\boldsymbol{K}$

$$R_{\boldsymbol{K}^{\mathrm{T}}\boldsymbol{K}}(\boldsymbol{X}) = \frac{\boldsymbol{X}^{\mathrm{T}}(\boldsymbol{K}^{\mathrm{T}}\boldsymbol{K})\boldsymbol{X}}{\boldsymbol{X}^{\mathrm{T}}\boldsymbol{X}} = \frac{|\boldsymbol{K}\boldsymbol{X}|^2}{|\boldsymbol{X}|^2} = \frac{|\boldsymbol{F}|^2}{|\boldsymbol{X}|^2} \qquad (16)$$

Let $G_{\boldsymbol{K}}(\boldsymbol{X}) = \sqrt{R_{\boldsymbol{K}^{\mathrm{T}}\boldsymbol{K}}(\boldsymbol{X})}$, $G_{\boldsymbol{K}}(\boldsymbol{X})$ is defined as static stiffness performance quotient, then

$$|\boldsymbol{F}| = G_{\boldsymbol{K}}(\boldsymbol{X})|\boldsymbol{X}| \qquad (17)$$

According to Equation (17), when the external force $\boldsymbol{F}$ is given, the larger $G_{\boldsymbol{K}}(\boldsymbol{X})$ is, the stronger the resistance to deformation of the manipulator is, and vice versa. The properties of $G_{\boldsymbol{K}}(\boldsymbol{X})$ can be obtained by studying the eigenvalues of $\boldsymbol{K}^{\mathrm{T}}\boldsymbol{K}$. According to the symmetry and positive definiteness of $\boldsymbol{K}^{\mathrm{T}}\boldsymbol{K}$, its eigenvalues satisfy $\lambda_i > 0$ $(i = 1, 2, \cdots, n)$. Let $\lambda_1 \leq \lambda_2 \leq \cdots \leq \lambda_n$ and $G_i = \sqrt{\lambda_i}$, it's clear that G_i is the singular value of matrix $\boldsymbol{K}$ according to the definition of singular value. It can be proved that the static stiffness performance quotient satisfies the inequality.

$$G_1 \leq G_{\boldsymbol{K}}(\boldsymbol{X}) \leq G_n \qquad (18)$$

Take the minimum singular value of the stiffness matrix $\boldsymbol{K}$ as $G_1 = \sigma_{\min}(\boldsymbol{K})$. For the whole workspace, the manipulator end has the weakest stiffness at the position with the minimum singular value, where the deformation of the anthropomorphic manipulator end is the largest. Therefore, the minimum singular value $G_1 = \sigma_{\min}(\boldsymbol{K})$ can be used as an evaluation index of stiffness performance. The greater the minimum singular value is, the better the corresponding stiffness is. So, the optimization goal is to make the minimum singular value be maximized.

C. COMPREHENSIVE PERFORMANCE INDEXES OF ANTHROPOMORPHIC MANIPULATOR

Considering the three indexes, Jacobian matrix condition number, manipulability, and stiffness performance, a comprehensive performance index η of the anthropomorphic manipulator was established.

$$\eta = \frac{w^\beta \sigma_{\min}^\gamma(\boldsymbol{K})}{k_F^\alpha} \qquad (19)$$

where, k_F, w, $\sigma_{\min}(\boldsymbol{K})$ respectively represent the Jacobian matrix condition number, manipulability, and the minimum singular value of the stiffness matrix. The α, β and γ are the corresponding weight coefficients, satisfying $\alpha + \beta + \gamma = 1$. In the design and optimization process of the anthropomorphic manipulator, the weight coefficients (α, β, γ) can be determined according to the actual task and application requirements. The evaluation index comprehensively considers the isotropy, manipulability and end stiffness of the anthropomorphic manipulator. The larger the value of η is, the more isotropic the manipulator tends to be, and the better the manipulability is. Moreover, the larger the minimum singular value of the stiffness matrix is, the better the stiffness performance is. Substituting the calculation formula of k_F, w, $\sigma_{\min}(\boldsymbol{K})$ into the expression of comprehensive performance

TABLE 3. The constraints on joints and the link length.

Constraint type	Angle constraints	Link length constraints
Constraints	$s.t.\begin{cases} -60° \leq \theta_1 \leq 160° \\ -20° \leq \theta_2 \leq 160° \\ 20° \leq \theta_3 \leq 160° \\ -20° \leq \theta_4 \leq 160° \\ -100° \leq \theta_5 \leq 100° \\ -100° \leq \theta_6 \leq 100° \\ -40° \leq \theta_7 \leq 80° \end{cases}$	$s.t.\begin{cases} 150mm \leq d_1 \leq 250mm \\ 200mm \leq d_2 \leq 400mm \\ 200mm \leq d_3 \leq 400mm \\ 100mm \leq d_4 \leq 250mm \\ d_1 + d_2 + d_3 + d_4 = 979mm \end{cases}$

index, we can obtain

$$\eta = \frac{\left(\sqrt{\det\left(\boldsymbol{JJ}^{\mathrm{T}}\right)}\right)^{\beta}\left(\sigma_{\min}\left(\left(\boldsymbol{JJ}^{\mathrm{T}}\right)^{-\mathrm{T}}\boldsymbol{JK}_q\boldsymbol{J}^{\mathrm{T}}\left(\boldsymbol{JJ}^{\mathrm{T}}\right)^{-1}\right)\right)^{\gamma}}{\left(\frac{1}{6}\sqrt{tr\left(\boldsymbol{JJ}^{\mathrm{T}}\right)tr\left[\left(\boldsymbol{JJ}^{\mathrm{T}}\right)^{-1}\right]}\right)^{\alpha}}$$

(20)

Let $\boldsymbol{M} = \boldsymbol{JJ}^{\mathrm{T}}$, then

$$\eta = \frac{\left(\sqrt{\det\left(\boldsymbol{M}\right)}\right)^{\beta}\left(\sigma_{\min}\left(\boldsymbol{M}^{-\mathrm{T}}\boldsymbol{JK}_q\boldsymbol{J}^{\mathrm{T}}\boldsymbol{M}^{-1}\right)\right)^{\gamma}}{\left(\frac{1}{6}\sqrt{tr\left(\boldsymbol{M}\right)tr\left(\boldsymbol{M}^{-1}\right)}\right)^{\alpha}}$$

(21)

In order to measure the motion performance of the anthropomorphic manipulator, the comprehensive performance evaluation function η is integrated in the whole reachable workspace, and the global comprehensive performance index f in the workspace is obtained, which can be expressed as

$$f = \frac{\int_W \eta dW}{\int_W dW} = \frac{\int_\psi \eta d\theta_1 d\theta_2 \cdots d\theta_n}{\int_\psi d\theta_1 d\theta_2 \cdots d\theta_n}$$

(22)

f is the global comprehensive performance index of the manipulator, which can be used to evaluate the average motion performance of the manipulator in the whole reachable workspace. Where, η is the comprehensive performance index, W is the reachable workspace of the manipulator, ψ is the joint space, θ_i is the joint angles of the manipulator ($i = 1, 2, \cdots, n$).

IV. LINK LENGTH PARAMETERS OPTIMIZATION OF ANTHROPOMORPHIC MANIPULATOR

A. ESTABLISHMENT OF OPTIMIZATION MODEL

The link length parameters optimization is to find a group of optimal link lengths to achieve the best motion performance of the manipulator within the constraint range of manipulator length. The global comprehensive performance index f of the anthropomorphic manipulator is a function of the link lengths $l_1, l_2, \cdots l_n$. When f reaches the maximum value, the corresponding link lengths are the optimal. Therefore, the reciprocal of f can be used as the link lengths optimization objective function of the manipulator. Let

$$g(l_1, l_2, \ldots l_n) = \frac{1}{f(l_1, l_2, \ldots l_n)}$$

(23)

So, the optimization model is established as follows

$$\min g(l_1, l_2, \cdots l_n)$$
$$s.t. \begin{cases} \theta_{i\min} \leq \theta_i \leq \theta_{i\max} \\ l_{i\min} \leq l_i \leq l_{i\max} \\ l_1 + l_2 + \cdots + l_n = L \end{cases} \quad (i = 1, 2 \cdots n)$$

According to the kinematics model of the manipulator, the link length variables in the Jacobian matrix can be expressed by d_1, d_2, d_3 and d_4 (where, $d_1 = l_1 + l_2$, $d_2 = l_3 + l_4$, $d_3 = l_5 + l_6$ and $d_4 = l_7$). The optimization model can be simplified as

$$\min g(d_j)$$
$$s.t. \begin{cases} \theta_{i\min} \leq \theta_i \leq \theta_{i\max} & (i = 1, 2 \cdots 7) \\ d_{j\min} \leq d_j \leq d_{j\max} & (j = 1, 2 \cdots 4) \\ d_1 + d_2 + d_3 + d_4 = L \end{cases}$$

In the design process of an anthropomorphic manipulator, the joint motion range is usually set to be slightly larger than the actual joint motion range of human arm. The motion constraints of each joint of the manipulator can be determined according to the data in Table 1. The constraints on the link lengths are determined by the actual design requirements. The total length of the manipulator is set to $L = 979$ mm according to the actual operation requirements and the required workspace. The constraints on the anthropomorphic manipulator link lengths are calculated according to the dimensions of the joint drive and transmission components, as shown in Table 3.

B. SOLUTION OF OPTIMIZATION MODEL

According to the performance parameters of the driving and transmission parts, the stiffness of each joint is $K_{q1} = K_{q2} = 6.7e5 \ N \cdot m/rad$, $K_{q3} = K_{q4} = 3.1e4 \ N \cdot m/rad$, $K_{q5} = K_{q6} = 5.8e3 \ Nm/rad$ and $K_{q7} = 2.9e3 \ N \cdot m/rad$, and the joint stiffness matrix is (unit is $N \cdot m/rad$):

$$K_q = diag\left(6.7e5 \ 6.7e5 \ 3.1e4 \ 3.1e4 \ 5.8e3 \ 5.8e3 \ 2.9e3\right)$$

The expression of global comprehensive performance index is as follows

$$f = \frac{\int_W \eta dW}{\int_W dW} = \frac{\int_\psi \frac{w^\beta \sigma_{\min}^\gamma(\boldsymbol{K})}{k_F^\alpha} d\theta_1 d\theta_2 \cdots d\theta_n}{\int_\psi d\theta_1 d\theta_2 \cdots d\theta_n}$$

(24)

TABLE 4. Optimized link lengths and corresponding performance indexes.

α, β, γ	d_1^*	d_2^*	d_3^*	d_4^*	f_k	f_w	f_σ	f
$\alpha = 1, \beta = \gamma = 0$	250.0	399.9	200.0	129.1	67.91	0.0540	2.235e3	0.0147
$\beta = 1, \alpha = \gamma = 0$	250.0	400.0	229.0	100.0	74.59	0.0559	2.231e3	0.0559
$\gamma = 1, \alpha = \beta = 0$	200.2	300.5	295.7	182.6	104.32	0.0311	2.324e3	2324.3

Combining the known conditions and constraints, the specific value of the weight coefficients should be determined according to the tasks and application requirements of the manipulator when solving the optimization model. Since the Jacobian matrix condition number and the manipulability are both indexes to characterize the flexibility of the manipulator, and the minimum singular value of stiffness matrix is the index that characterizes the end stiffness. Therefore, the optimized link length parameters will change with different weight coefficients, and the corresponding manipulator has different flexibility and end stiffness performance. In order to explore the influence of the weight coefficients on various performance indexes of the manipulator, the global condition number, global manipulability and global stiffness performance are considered separately. The optimizations are performed by using the LM (Levenberg-Marquardt) algorithm in three cases: $\alpha = 1$, $\beta = \gamma = 0$, $\beta = 1, \alpha = \gamma = 0$ and $\gamma = 1, \alpha = \beta = 0$, where

$$f_k = \frac{\int\limits_W k_F dW}{\int\limits_W dW}, (\alpha = 1, \beta = \gamma = 0) \qquad (25)$$

$$f_w = \frac{\int\limits_W w dW}{\int\limits_W dW}, (\beta = 1, \alpha = \gamma = 0) \qquad (26)$$

$$f_\sigma = \frac{\int\limits_W \sigma_{\min}(K) dW}{\int\limits_W dW}, (\gamma = 1, \alpha = \beta = 0) \qquad (27)$$

The optimized link lengths and the corresponding performance indexes values are shown in Table 4, from which it can be seen that the global condition number index f_k takes the minimum value $f_{k\,\min} = 67.91$ when considering the global condition number only. The global manipulability index f_w takes the maximum value $f_{w\,\max} = 0.0559$ when considering the global manipulability only. The global stiffness performance index f_σ takes the maximum value $f_{\sigma\,\max} = 2.324e3$ when the stiffness performance is considered only.

When a certain performance index is considered separately for optimization, the optimal value of the corresponding performance can be obtained, while the motion performance corresponding to the other two indexes is relatively poor. Therefore, in order to balance the flexibility and stiffness of the manipulator, take $\alpha = \beta = 0.25$, $\gamma = 0.5$. The optimal solution for the link lengths was obtained as follows $d_1^* = 226.7mm, d_2^* = 379.4mm, d_3^* = 245.3mm, d_4^* = 127.6mm$

TABLE 5. The initial design lengths and optimized lengths of the links.

The initial design lengths (mm)		The optimized lengths (mm)
l_1=108.5 l_2=110.5	d_1=219.0	$d_1^* = 226.7$
l_3=199.5 l_4=110.5	d_2=310.0	$d_2^* = 379.4$
l_5=199.5 l_6=81.5	d_3=281.0	$d_3^* = 245.3$
l_7=169.0	d_4=169.0	$d_4^* = 127.6$
L=979	$d_1 + d_2 + d_3 + d_4 = d_1^* + d_2^* + d_3^* + d_4^*$	

TABLE 6. Comparison of various global performance indexes.

Index type	Initial lengths d	Optimized lengths d^*	Rate of change
f_k	100.96	78.61	-22.14%
f_w	0.0365	0.0457	25.21%
f_σ	2.273e3	2.256e3	-0.75%
f	6.7659	8.3752	23.79%

The solution $g_{\min} = 0.1194$ is obtained, and the corresponding global comprehensive performance index f takes the maximum value $f_{\max} = 8.3752$.

C. SIMULATION VERIFICATION AND COMPARATIVE ANALYSIS

According to the proposed global performance index f, the length parameters of the manipulator are optimized under the premise that the overall length is determined when $\alpha = \beta = 0.25$ and $\gamma = 0.5$. The initial design lengths and the optimized lengths of the links are shown in Table 5.

Based on the two groups of link lengths before and after optimization, the motion performance of the manipulator is compared. The global condition number f_k, global manipulability f_w, global stiffness performance index f_σ and global comprehensive performance index f before and after optimization are calculated, and the specific values are shown in Table 6.

Through simulations and calculations, the global comprehensive performance indexes before and after the optimization are $f = 6.7659$ and $f^* = 8.3752$. The index value increased by about **23.79%**, where, the global condition number index value is reduced by 22.14%, the global manipulability index value increased by 25.21%, and the global stiffness performance index value has a smaller change
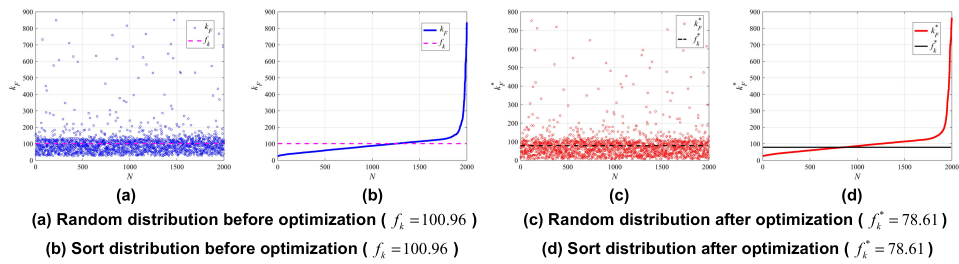
FIGURE 5. The distribution of global condition number before and after optimization.
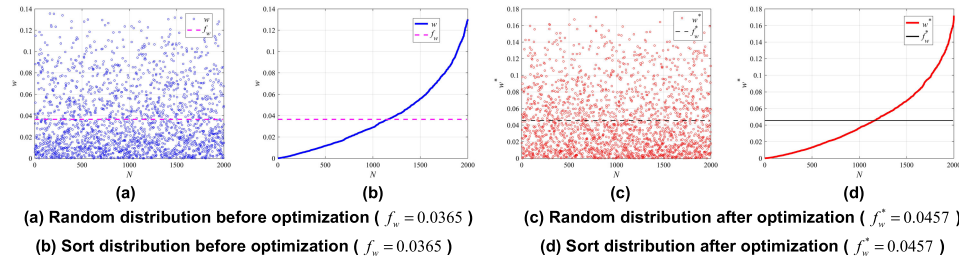
(a) Random distribution before optimization ($f_k = 100.96$)
(b) Sort distribution before optimization ($f_k = 100.96$)
(c) Random distribution after optimization ($f_k^* = 78.61$)
(d) Sort distribution after optimization ($f_k^* = 78.61$)

FIGURE 6. The distribution of global manipulability before and after optimization.

(a) Random distribution before optimization ($f_w = 0.0365$)
(b) Sort distribution before optimization ($f_w = 0.0365$)
(c) Random distribution after optimization ($f_w^* = 0.0457$)
(d) Sort distribution after optimization ($f_w^* = 0.0457$)
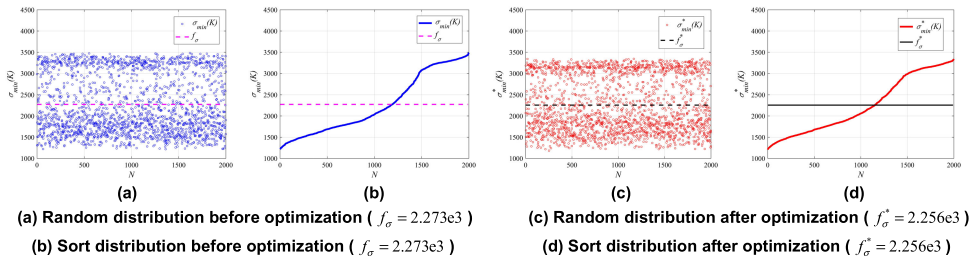
FIGURE 7. The distribution of stiffness performance before and after optimization.

(a) Random distribution before optimization ($f_\sigma = 2.273e3$)
(b) Sort distribution before optimization ($f_\sigma = 2.273e3$)
(c) Random distribution after optimization ($f_\sigma^* = 2.256e3$)
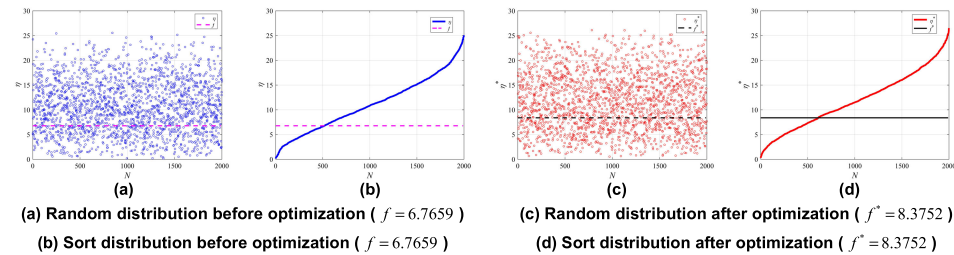(d) Sort distribution after optimization ($f_\sigma^* = 2.256e3$)

FIGURE 8. The distribution of global comprehensive performance index before and after optimization.

(a) Random distribution before optimization ($f = 6.7659$)
(b) Sort distribution before optimization ($f = 6.7659$)
(c) Random distribution after optimization ($f^* = 8.3752$)
(d) Sort distribution after optimization ($f^* = 8.3752$)
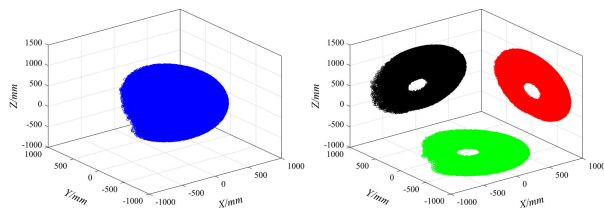

FIGURE 9. Workspace of the manipulator before optimization.
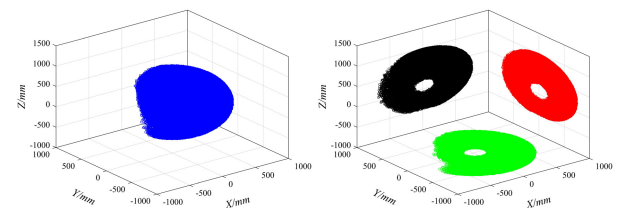

FIGURE 10. Workspace of the manipulator after optimization.

with a decrease of about 0.75%. Taking 2000 groups of joint angles in the joint space of the manipulator and calculating the corresponding end coordinates, the distributions of the global performance indexes of the manipulator at 2000 points before and after the optimization are shown in FIGUREs 5-8.

From FIGUREs 5-8, it can be seen that the global condition number, global manipulability and global comprehensive performance have been improved to some extent after optimization. The distributions of various indexes values in the workspace before and after optimization are basically

TABLE 7. Comparison of the workspace boundaries before and after optimization.

manipulator length	X/[mm]		Y/[mm]		Z/[mm]	
	min	max	min	max	min	max
Initial length d	-698.9	757.9	-758.4	736.5	-515.3	979.0
Optimized length d^*	-691.1	750.4	-752.2	722.6	-499.2	979.0

(a) Global Jacobian condition number

(b) Global manipulability

(c) Global stiffness performance index

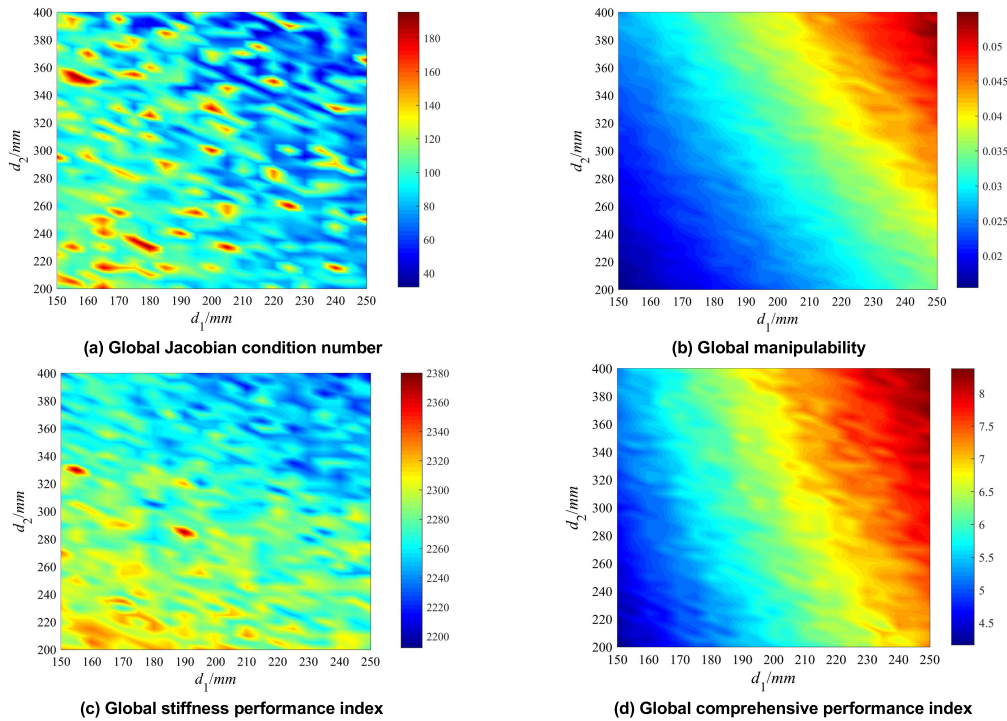(d) Global comprehensive performance index

FIGURE 11. Variations of various motion performance with d_1 and d_2.

consistent, and the comprehensive motion performances have been significantly improved. Through the above analysis, it can be seen that the manipulator has the best comprehensive motion performance when satisfying $l_1^* + l_2^* = d_1^*$, $l_3^* + l_4^* = d_2^*$, $l_5^* + l_6^* = d_3^*$ and $l_7^* = d_4^*$, when $\alpha = \beta = 0.25$ and $\gamma = 0.5$. By changing the weight coefficients α, β, γ, the link lengths of anthropomorphic manipulator with different performance requirements can be optimized. In addition, the workspace and its sectional projection corresponding to the initial design lengths and optimized lengths are shown in FIGURE 9 and FIGURE 10, and the boundary values of the workspace are shown in Table 7.

According to the data in Table 7, the workspace decreases by 1.05%, 1.34% and 1.08% in X, Y and Z directions after the optimization, but the amounts of changes are small. The workspace of the manipulator is basically the same before and after the optimization.

D. ANALYSIS OF THE INFLUENCE OF LINK LENGTH ON MOTION PERFORMANCE

According to the data in Table 4, d_1 and d_2 take the maximum value and d_3 takes the minimum value when considering the global condition number only. d_1 and d_2 take the maximum value and d_4 takes the minimum value when considering the global manipulability only. The values of d_1 and d_2 decrease and the values of d_3 and d_4 increase when the stiffness performance is considered only. In order to explore the influence of d_1 and d_2 on various performance indexes, set $\alpha = \beta = 0.25$ and $\gamma = 0.5$, and calculate the values of various global performance indexes for different $d_1 \in [150, 250]mm$ and $d_2 \in [200, 400]mm$. The calculation results are shown in FIGURE 11. There is a certain correlation between each global performance index and d_1 and d_2. With the increase of d_1 and d_2, the Jacobian matrix condition number becomes smaller, the value of manipulability increases, the stiffness performance index decreases slightly, and the global comprehensive performance index increases. The comprehensive motion performance of the manipulator has been improved. Therefore, in the design process of the anthropomorphic manipulator, d_1 and d_2 can be adjusted to make the motion performance meet the actual task requirements when satisfying the constraints of link lengths.

V. CONCLUSION

How to determine the optimal link length parameters according to task requirements and constraints is a key problem

in the design of anthropomorphic manipulators. Aiming at this problem, this article analyzes the optimal configuration of anthropomorphic manipulator based on the structure and motion mechanism of human arm, establishes the kinematics model using the screw theory, and proposes a comprehensive evaluation index considering the Jacobian matrix condition number, manipulability and manipulator end stiffness. The length parameters optimization model of the anthropomorphic manipulator is established, and the link lengths of a manipulator with both flexibility and stiffness are optimized. The correctness and rationality of the proposed optimization model are verified through comparisons and analyses. The conclusions are as follows:

(1) Using screw theory, the kinematics model of a anthropomorphic manipulator with seven DOFs is established, and the end stiffness matrix of the manipulator is derived. The minimum singular value of the stiffness matrix can be used as the performance index to evaluate the end stiffness.

(2) A global comprehensive performance index is established considering the Jacobian matrix condition number, manipulability and end stiffness of the anthropomorphic manipulator. The link lengths of the anthropomorphic manipulator with different performance and requirements can be optimized by changing the weight coefficients.

(3) The optimal link length was obtained, and the global comprehensive performance index value of the manipulator has increased by about 23.79% after optimization. Its comprehensive motion performance has been significantly improved, which proves the correctness and rationality of the optimization method. The influence of the relative lengths of the links on each performance index are analyzed when the total length is given, which provides a theoretical basis for the design of anthropomorphic manipulators.

REFERENCES

[1] J. Zhao, C. Y. Song, and B. Du, "Configuration of humanoid robotic arm based on human engineering," *J. Mech. Eng.*, vol. 49, no.11, pp. 16–21, Jun. 2013.

[2] W. Liu, D. Chen, and J. Steil, "Analytical inverse kinematics solver for anthropomorphic 7-DOF redundant manipulators with human-like configuration constraints," *J. Intell. Robot. Syst.*, vol. 86, no. 1, pp. 63–79, Dec. 2016.

[3] S. N. Nabavi, M. Shariatee, J. Enferadi, and A. Akbarzadeh, "Parametric design and multi-objective optimization of a general 6-PUS parallel manipulator," *Mechanism Mach. Theory*, vol. 152, Oct. 2020, Art. no. 103913.

[4] D. H. Lee, H. Park, J.-H. Park, M. H. Baeg, and J. H. Bae, "Design of an anthropomorphic dual-arm robot with biologically inspired 8-DOF arms," *Intell. Service Robot.*, vol. 10, no. 2, pp. 1–12, Jan. 2017.

[5] P. Zhang, Z. Yao, and Z. Du, "Global performance index system for kinematic optimization of robotic mechanism," *J. Mech. Des.*, vol. 136, no. 3, Mar. 2014, Art. no. 031001.

[6] W. A. Khan and J. Angeles, "The kinetostatic optimization of robotic manipulators: The inverse and the direct problems," *J. Mech. Des.*, vol. 128, no. 1, pp. 166–178, Jan. 2006.

[7] S.-G. Kim and J. Ryu, "New dimensionally homogeneous Jacobian matrix formulation by three end-effector points for optimal design of parallel manipulators," *IEEE Trans. Robot. Autom.*, vol. 19, no. 4, pp. 731–736, Aug. 2003.

[8] H.-G. Kim, K.-S. Shin, S.-W. Hwang, and C.-S. Han, "Link length determination method for the reduction of the performance deviation of the manipulator: Extension of the valid workspace," *Int. J. Precis. Eng. Manuf.*, vol. 15, no. 9, pp. 1831–1838, Sep. 2014.

[9] P. Larochelle, "Synthesis of part orienting devices for spatial assembly tasks," in *Proc. 11th Interpretational Symp. Adv. Robot Kinematics*. Batz-sur-Mer, France: Spring-Verlag, Jun. 2008, pp. 79–87.

[10] S. Y. Jia, Y. H. Jia, and S. J. Xu, "Dimensional optimization method for manipulator based on orientation manipulability," *J. Beijing Univ. Aeronaut. Astronaut.*, vol. 41, no. 9, pp. 1693–1700, Sep. 2015.

[11] Y. Hwang and J. Yoon, "The optimum design of a 6-DOF parallel manipulator with large orientation workspace," in *Proc. Int. Conf. Robot. Autom.*, May 2007, pp. 163–168.

[12] S. Hwang, H. Kim, Y. Choi, K. Shin, and C. Han, "Design optimization method for 7 DOF robot manipulator using performance indices," *Int. J. Precis. Eng. Manuf.*, vol. 18, no. 3, pp. 293–299, Mar. 2017.

[13] H. Lim, S. Hwang, K. Shin, and C. Han, "Comparative study of optimization technique for the global performance indices of the robot manipulator based on an approximate model," *Int. J. Control, Autom. Syst.*, vol. 10, no. 2, pp. 374–382, Apr. 2012.

[14] Y. J. Liu, X. X. Xu, and T. Huang, "Workspace topologies and dimensional synthesis for biological detection manipulator," *J. Mech. Eng.*, vol. 51, no. 3, pp. 51–57, Jun. 2015.

[15] R. V. Mayorga, J. Carrera, and M. M. Oritz, "A kinematics performance index based on the rate of change of a standard isotropy condition for robot design optimization," *Robot. Auto. Syst.*, vol. 53, nos. 3–4, pp. 153–163, Dec. 2005.

[16] H. Liu, T. Huang, J. Mei, X. Zhao, D. G. Chetwynd, M. Li, and S. J. Hu, "Kinematic design of a 5-DOF hybrid robot with large workspace/limb–stroke ratio," *J. Mech. Des.*, vol. 129, no. 5, pp. 530–537, May 2007.

[17] A. Ajoudani, N. G. Tsagarakis, and A. Bicchi, "On the role of robot configuration in Cartesian stiffness control," in *Proc. IEEE Int. Conf. Robot. Autom. (ICRA)*, Seattle, WA, USA, May 2015, pp. 1010–1016.

[18] S. Chen, Y. Liu, P. Wu, J. Hu, Y. Guan, and G. Liu, "Arm link lengths optimization of robot on stiffness performance," *J. Mach. Electron.*, vol. 6, pp. 67–72, May 2015.

[19] J. Zhang, J. Yang, Y. Yue, K. Wen, and Y. Zhou, "Optimization of comprehensive stiffness performance index for industrial robot in milling process," in *Proc. IEEE 10th Int. Conf. Mech. Aerosp. Eng. (ICMAE)*, Brussels, Belgium, Jul. 2019, pp. 544–549.

[20] J. C. Jiao, W. Tian, and Z. H. Shi, "A robotic configuration optimization method based on redundancy freedom," *J. Aerosp. Manuf. Technol.*, vol. 61, no. 4, pp. 16–21, Apr. 2018.

[21] W. Chen, J. Chen, C. Hu, and Q. Chen, "Stiffness analysis and optimization of a novel cable-driven anthropomorphic-arm manipulator," *J. Huazhong Univ. Sci. Tech. (Natural Sci. Ed.)*, vol. 41, no. 2, pp. 12–16, Feb. 2013.

[22] A. Klimchik, Y. Wu, A. Pashkevich, S. Caro, and B. Furet, "Optimal selection of measurement configurations for stiffness model calibration of anthropomorphic manipulators," *Appl. Mech. Mater.*, vol. 162, pp. 161–170, Mar. 2012.

[23] R. A. Prokopenko, A. A. Frolov, E. V. Biryukova, and A. Roby-Brami, "Assessment of the accuracy of a human arm model with seven degrees of freedom," *J. Biomechanics*, vol. 34, no. 2, pp. 177–185, Feb. 2001.

[24] I. Kuhlemann, P. Jauer, F. Ernst, and A. Schweikard, "Robots with seven degrees of freedom: Is the additional DoF worth it?" in *Proc. 2nd Int. Conf. Control, Autom. Robot. (ICCAR)*, Apr. 2016.

[25] F. Zacharias, I. S. Howard, T. Hulin, and G. Hirzinger, "Workspace comparisons of setup configurations for human-robot interaction," in *Proc. IEEE/RSJ Int. Conf. Intell. Robots Syst.*, Nov. 2010, pp. 3117–3122.

[26] J. K. Salisbury and J. J. Craig, "Articulated hands: Force control and kinematic issues," *Int. J. Robot. Res.*, vol. 1, no. 1, pp. 4–17, Mar. 1982.

[27] T. Yoshikawa, "Manipulability of robotic mechanisms," *Int. J. Robot. Res.*, vol. 4, no. 2, pp. 3–9, Jun. 1985.

[28] E. Abele, M. Weigold, and S. Rothenbücher, "Modeling and identification of an industrial robot for machining applications," *CIRP Ann.-Manuf. Technol.*, vol. 56, no. 1, pp. 387–390, Mar. 2007.

[29] Y. Bu, W. Liao, W. Tian, J. Zhang, and L. Zhang, "Stiffness analysis and optimization in robotic drilling application," *Precis. Eng.*, vol. 49, pp. 388–400, Jul. 2017.

QINHUAN XU received the B.E. degree in material forming and control engineering from the Shandong University of Science and Technology, Jinan, China, in 2011, and the M.E. degree in mechanical design and automation from the Jiangsu University of Science and Technology, Zhenjiang, China, in 2014. He is currently pursuing the Ph.D. degree in mechanical engineering with the Robotics Institute, Beihang University, Beijing, China.

His research interests include redundant manipulator kinematics and mechanism design. His awards and honors include the four First Grade Undergraduate Scholarships, the "Three Good" Student of the Shandong University of Science and Technology, the Beijing Zhongkuang Scholarship, the People Scholarship, and the Excellent Graduate Student.

QIANG ZHAN received the B.E. degree in mechanical engineering and the D.E. degree in mechatronic engineering from the Harbin Institute of Technology, Harbin, China, in 1995 and 1999, respectively.

From 1999 to 2001, he was a Postdoctoral Researcher with the Robotics Institute, Beihang University (previously the Beijing University of Aeronautics and Astronautics), Beijing, China, where he became an Associate Professor in 2002 and a Full Professor in 2009. He was a Visiting Professor with the Ecole Centrale de Lille, France, in 2011, and Cranfield University, U.K., in 2015. He is the author or a coauthor of four books, more than 100 articles, and more than ten inventions. His research interests include robotic hands, spherical robot, mechanism design, and motion control of robotic systems. His awards and honors include the Silver Award of the 17th National Invention Exhibition of China, the AVIC Science and Technology Award, the Annual Excellent Paper of Chinese Mechanical Engineering Society, and the Annual Excellent Paper of Chinese Society of Astronautics. He is a member of the editorial committees of *Journal of Beijing University of Aeronautics and Astronautics*, *Journal of Harbin Institute of Technology*, and *Journal of Harbin Engineering University*.

XINYANG TIAN received the B.E. degree in mechanical engineering from Northeast Agricultural University, Harbin, China, in 2016. He is currently pursuing the Ph.D. degree with the Robotics Institute, Beihang University.

His research interests include modular joint and redundant manipulator. His awards and honors include the Special Prize of the Second National TRIZ Cup of Innovation Method Competition, the First Prize of the National Mathematical Modeling Competition for College Students of Heilongjiang Province, the First Prize of the 14th "Challenge Cup" College Students Extracurricular Academic Science and Technology Works Competition of Heilongjiang Province, the Third Prize of the 14th "Challenge Cup" National College Students Extracurricular Academic Science and Technology Works Competition, the Second Prize of the 13th "Huawei Cup" National Graduate Students Mathematics Modeling Competition, and the Merit Student of Heilongjiang Province.

. . .